Hindawi
Discrete Dynamics in Nature and Society
Volume 2018, Article ID 5027958, 15 pages
https://doi.org/10.1155/2018/5027958

Research Article

A New Formulation on Seismic Risk Assessment for Reinforced Concrete Structures with Both Random and Bounded Uncertainties

Xiao-Xiao Liu [1] **and Yuan-Sheng Wang** [2]

[1] *State Key Laboratory for Strength and Vibration of Mechanical Structures, School of Aerospace, Xi'an Jiaotong University, Xi'an 710049, China*
[2] *Department of Mechanical and Civil Engineering, Northwestern Polytechnical University, Xi'an 710129, China*

Correspondence should be addressed to Xiao-Xiao Liu; xxliu1989@xjtu.edu.cn
and Yuan-Sheng Wang; wangyuansheng@nwpu.edu.cn

Received 13 July 2018; Accepted 18 September 2018; Published 1 November 2018

Academic Editor: Allan C. Peterson

A new formulation on seismic risk assessment for structures with both random and uncertain-but-bounded variables is investigated in this paper. Limit thresholds are regarded as random variables. The median of random variables is described through an improved multidimensional parallelepiped (IMP) convex model, in which the uncertain domain of the dependent bounded variables can be explicitly expressed. The corresponding Engineering Demand Parameters are taken to be dependent and follow a multidimensional lognormal distribution. Through matrix transformation, a given performance function is transformed into the regularized one. An effective method based on active learning Kriging model (ALK) is introduced to approximate the performance function in the region of interest rather than in the overall uncertain space. Based on ALK model, the failure probabilities for different limit states are calculated by using Monte Carlo Simulation (MCS). Further, the failure probabilities for different limit states in 50 years can be obtained through coupling the seismic failure probability with the ground motion hazard curve. A six-story reinforced concrete building subjected to ground motions is investigated to the efficiency and accuracy of the proposed method. The interstory drift and the acceleration as two responses of the case study are, respectively, obtained by utilizing Incremental Dynamic Analysis and nonlinear history analysis.

1. Introduction

Recent earthquake hazards have caused serious economic and social loss [1, 2]. Currently, a number of academics [3–7] have emphasized the importance of performance-based seismic design (PBSD). A large amount of approaches for reliability analysis of structures has been proposed in recent years. Limit state fragility curves as considerable decision-making tools have been proposed to assess the reliability of RC structures [8–14]. The well-known Cornell's three analytical seismic risk formulae have been widely used to carry out structural seismic reliability analysis [15, 16]. For instance, Eads et al. [17] used these analytical risk formulations to estimate collapse risk of a four-story office building. In Lu et al. [18, 19] the structural seismic hazard analysis could be studied by combining an improved cloud method and the analytical formulation of the damage hazard. Lü et al. [20] also applied Cornell's three analytical seismic risk formulae to evaluate the seismic reliability of Chinese code-conforming buildings. In Wu et al. [21] the seismic risk assessment of RC buildings subjected to near-fault and far-fault ground motions was investigated using Cornell's three analytical formulations. Moreover, the finite element reliability module based on the first-order reliability method (FORM) and MVFOSM has been proposed for seismic reliability problems [18, 19, 22, 23]. Song et al. [24] developed a component reliability method to identify the most probable failure members of RC buildings subjected to strong ground motions. Then the probability of a progressive collapse of the damaged structures could be calculated by the integral reliability method. Lü et al. [25]

proposed a semi-analysis approach integrating the improved point method and moment method to analyze the nonlinear seismic reliability of a specific structure. The applicability of the reliability methodologies such as FORM, SORM, and HOMM was elaborated by Song [26] and Lu et al. [27]. Note that all of these reliability methods were based on the framework of performance-based seismic design (PBSD).

However, the above-mentioned contributions are usually based on specific probability distributions of uncertain variables, which may be imprecise for some uncertain parameters because of insufficient experimental data. Unreasonable assumptions may cause misleading results in probabilistic reliability analysis [28, 29], if a probabilistic model is adopted. Therefore, the nonprobabilistic convex model was presented to describe the uncertain parameters with the limited available information. In the last several years, the structural reliability analysis methods based on the nonprobabilistic convex models have been intensively investigated [30–33] and they have provided effective supplements to traditional probabilistic reliability analysis. Moreover, the structural hybrid reliability analysis with both random uncertainty and bounded uncertainty has been proposed in recent years [34–36].

Guo and Du [37] developed a unified reliability analysis framework to deal with both random and interval variables in multidisciplinary systems. Jiang et al. [38] constructed an algorithm with high efficiency and robust convergence performance to compute the hybrid reliability with both random and interval variables. Recently, an improved unified analysis approach [39] for structural hybrid reliability has been developed based on FORM. Moreover, sensitivity analysis for hybrid reliability with both probabilistic and convex variables was investigated in Guo and Du [34, 40], Wang et al. [41], and Zhang et al. [42, 43]. In Luo et al. [35], a probability and convex set mixed reliability model was proposed. Subsequently, the minimum reliability index was used as the constraint in reliability-based design optimization (RBDO) when both random and convex variables were considered. Yang et al. [44, 45] demonstrated that if performance functions were highly nonlinear or had multiple design points, the existing algorithms [38, 46] (Xiao et al., 2006) would be very inaccurate. To overcome the above problems, a number of scholars presented an active learning Kriging model (ALK) for hybrid reliability analysis [43–45, 47, 48]. When the Kriging model is constructed, the performance function need not be approximated throughout the uncertain space, but only in some region of interest.

It is noteworthy that traditional convex models such as interval model and ellipsoidal model are found not capable of dealing with complex "multisource uncertainty" problems. Therefore, a more general convex model, namely, "multidimensional parallelepiped (MP) model", was proposed in recent work [49–51]. This kind of convex model can take into account the independent and dependent uncertain parameters in a unified framework. To remedy the scarcity of the existing MP model, Ni et al. [52] presented an improved MP (IMP) model, in which the uncertainty domain of the interval variables could be explicitly expressed by a matrix inequality.

In conclusion, based on the framework of PBSD, the reliability analysis of a given RC structure subjected to ground motions should be discussed with a combination of probability and IMP convex models. This means that a more general hybrid reliability analysis (MGHAR) for complex seismic engineering problems is developed in this paper. Limit thresholds are considered as random variables. The median of random variables is expressed by using the IMP model. The structural responses are taken to be dependent and follow a multidimensional lognormal distribution. Through matrix transformation, the performance function is mapped into the normalized performance function. A method based on ALK model named ALK-MGHAR is proposed. The reason is that a surrogate only rightly predicting the sign of the performance function is found capable of satisfying the precision requirement of MGHAR. Then Monte Carlo Simulation (MCS) is efficiently performed based on ALK-MGHAR. Further, the failure probabilities in 50 years can be computed by combining seismic failure probability and the ground motion hazard curve. This procedure is called ALK-MGHAR-MCS. A six-story RC building is used to demonstrate the efficiency and accuracy of ALK-MGHAR. The interstory drift and the acceleration are selected as two-dimensional Engineering Demand Parameters (EDPs), which are, respectively, calculated by Incremental Dynamic Analysis (IDA) and nonlinear history analysis (NHA).

2. MGHAR with MCS Method

2.1. Seismic Risk Formulation with Probabilistic Model. When only random variables are involved in an uncertain structure, the reliability in conjunction with the PBSD approach can be evaluated by traditional probabilistic reliability method. The limit state function or performance function is expressed as $G(\mathbf{X})$, with the vector of random variables $\mathbf{X} = \{\boldsymbol{x}_1, \boldsymbol{x}_2, ..., \boldsymbol{x}_m\}$. The reliability is denoted as the probability that the structural response exceeds the specified damage level under a given ground motion intensity. In probabilistic reliability theory, therefore, the failure probability of a structure for a specific limit state can be defined as follows:

$$P_f = \Pr\{G(\mathbf{X}) < 0\} = \int_{G(\mathbf{X})<0} \cdots \int f(\mathbf{X})\, d\mathbf{X} \quad (1)$$

where P_f is the structural failure probability under a damage state, $\Pr\{\bullet\}$ represents the probability of an event, and $f(\mathbf{X})$ is the joint probability density function (PDF) of random variables $\mathbf{X}$. For normal random variables, $\mathbf{X}$ can be transformed into standard normal random variables $\mathbf{u}$ through a linear transformation, as follows:

$$u_i = \frac{x_i - \mu_i}{\sigma_i}, \quad (i = 1, 2, \ldots m) \quad (2)$$

where μ_i and σ_i are mean and standard deviation of random variables x_i, respectively.

For nonnormal random variables, numerous available techniques, such as Nataf transformation [57] and Rosenblatt's transformation [58], can transform the variables into approximately equivalent normal variables. Through such a treatment, the well-known FORM can be carried out for solving the structural reliability in (1).

In order to evaluate the reliability of RC buildings, the familiar Cornell approach [16] is adopted in this paper. The mean annual frequency (MAF) of exceeding a specified limit state per year is normally defined as

$$\lambda_{\mathrm{EDP}}(\mathrm{LS}) = \int_{IM} P_{\mathrm{EDP}|IM}(\mathrm{LS} \mid im) \left| \frac{\mathrm{d}H_{IM}(im)}{\mathrm{d}im} \right| \mathrm{d}im \quad (3)$$

where $P_{\mathrm{EDP}|IM}(\mathrm{LS} \mid im)$ is the structural failure probability for a specific limit state and can be solved through (1). $H_{IM}(im) = P[IM \geq im]$ is the ground motion hazard function and denotes the MAF of a specific earthquake event ($IM \geq im$); IM is the intensity measure (peak ground acceleration, spectral acceleration, etc.).

For specific site conditions, a simplified model proposed by Cornell et al. [15] can be used to carry out the ground motion hazard analysis, expressed as

$$H_{S_a}(x) = P[S_a > x] = k_0 \cdot x^{-k} \quad (4)$$

where k_0 is a constant depending on the ground motion characteristics, k is the slope of the seismic hazard curve in logarithmic coordinates, and S_a is spectral acceleration.

When earthquake occurrences in time are assumed to be a Poisson process [59], the failure probabilities for different limit states in 50 years are calculated by using the following expression:

$$P_{\mathrm{EDP}} = 1 - (1 - \lambda_{\mathrm{EDP}})^{50} \quad (5)$$

2.2. Seismic Risk Formulation with Both Random and Bounded Variables. When both random variables and IMP convex variables appear in an uncertain structure, the performance function can be denoted as $G(\mathbf{X}, \mathbf{Y})$, where $\mathbf{Y} = \{y_1, y_2, ..., y_m\}$ denotes the vector of marginal intervals and will be expounded in Section 3.2. The IMP convex variables are actually uncertain-but-bounded quantities. Due to the coexistence of random and bounded variables, the limit state $G(\mathbf{X}, \mathbf{Y}) = 0$ produces a cluster of limit state surfaces in the stochastic space. The minimum limit state, $\min G(\mathbf{X}, \mathbf{Y})$, which denotes the worst case of a given structure, is the most concerned in this study. A stringent reliability requirement can be satisfied only when the worst case is taken into account. For problems with both random and bounded variables, the failure probability of a structure for a specific limit state is defined as

$$\begin{aligned} P_{\mathrm{f}}^{\mathrm{U}} &= \Pr\left\{ \min_{\boldsymbol{Y}} \mathrm{G}(\mathbf{X}, \mathbf{Y}) < 0 \right\} \\ &= \int_{\min_{\mathbf{Y}} G(\mathbf{X},\mathbf{Y})<0} \cdots \int f(\mathbf{X}) \, \mathrm{d}\mathbf{X} \end{aligned} \quad (6)$$

where $P_{\mathrm{f}}^{\mathrm{U}}$ is the maximum failure probability when the minimum limit state is considered.

The reliability analysis of RC structures with both random and IMP variables can be investigated using (6). When the interstory drift and the acceleration are simultaneously considered, the performance function further elaborated in Section 3 is expressed as $G((\boldsymbol{\Delta}, \boldsymbol{\delta}), (\mathbf{D}, \mathbf{A}))$. In this performance function, threshold capacity values corresponding to the two EDPs are described as random variables. The median of random variables is represented by the IMP variables. The failure probability of structures subjected to earthquakes is expressed as

$$P_{\mathrm{f}}^{\mathrm{U}} = \iint_{\min_{\mu_{\boldsymbol{\alpha}}} G((\boldsymbol{\Delta},\boldsymbol{\delta}),(\mathbf{D},\mathbf{A}))} f(D, A \mid S_a = x) \, \mathrm{d}D \, \mathrm{d}A \quad (7)$$

where $P_{\mathrm{f}}^{\mathrm{U}}$ is the maximum failure probability corresponding to the minimum limit state $\min G((\boldsymbol{\Delta}, \boldsymbol{\delta}), (\mathbf{D}, \mathbf{A}))$, $f(\cdot)$ is the bivariate PDF, D is the interstory drift, A is the acceleration, and Δ and δ are threshold capacity values of the interstory drift and the acceleration, respectively.

For convenience, this subsection uses $\mathrm{M}(\mathbf{w})$ to replace the minimum value of the performance function $\min G((\boldsymbol{\Delta}, \boldsymbol{\delta}), (\mathbf{D}, \mathbf{A}))$. Then, the MAF of exceeding the two specific limit states per year is defined as

$$\begin{aligned} &\lambda_{D,A}(\Delta, \delta) \\ &= \int \iint_{\mathrm{M}(\mathbf{w})} f(D, A \mid S_a = x) \, \mathrm{d}D \, \mathrm{d}A \left| \frac{\mathrm{d}H_{S_a}(x)}{\mathrm{d}(x)} \right| |\mathrm{d}(x)| \\ &= \int \iint_{\mathrm{M}(\mathbf{w})} f(D, A \mid S_a = x) \, \mathrm{d}D \, \mathrm{d}A \left| h_{S_a}(x) \right| |\mathrm{d}(x)| \end{aligned} \quad (8)$$

where $H_{S_a}(\cdot)$ is the ground motion hazard function of the site derived from PHSA and S_a is the spectral acceleration. In this paper, MCS as the benchmark of ALK-MGHAR can be implemented to obtain an accurate result. Two steps required here are detailed as follows.

Step 1. A great deal of random samples involved in the performance function $G((\boldsymbol{\Delta}, \boldsymbol{\delta}), (\mathbf{D}, \mathbf{A}))$ is generated.

Step 2. An optimization problem elaborated in Section 4 is performed at each of the simulated samples. Subsequently, a failure indictor can be obtained at the corresponding sample.

Based on the above-mentioned two steps, (8) can be rewritten as

$$\begin{aligned} &\lambda_{D,A}(\Delta, \delta) \\ &= \int \iint_{\mathrm{M}(\mathbf{w})} f(D, A \mid S_a = x) \, \mathrm{d}D \, \mathrm{d}A \left| h_{S_a}(x) \right| |\mathrm{d}(x)| \\ &= \int \frac{1}{N_{\mathrm{MCS}}} \sum_{j=1}^{N} I_F\left(\mathbf{w}^{(j)}\right) \left| h_{S_a}(x) \right| |\mathrm{d}(x)| \end{aligned} \quad (9)$$

where $I_F(\mathbf{w})$ is the failure indictor function and it can be expressed as

$$I_F(\mathbf{w}) = \begin{cases} 1 & \mathrm{M}(\mathbf{w}) \geq 0 \\ 0 & \mathrm{M}(\mathbf{w}) < 0 \end{cases} \quad (10)$$

where $\mathrm{M}(\mathbf{w})$ is the minimum value of the performance function which can be elaborated in Section 3. In this paper, it should be noted that $\mathrm{M}(\mathbf{w}) \geq 0$ represents the failure region of a given structure and $\mathrm{M}(\mathbf{w}) < 0$ denotes the safe region.

Remark 1. (i) The failure probabilities in 50 years can be calculated by (5). (ii) Since the uncertainties in both responses originated from the same source of uncertainties, the two EDPs are taken to be dependent and follow a bivariate lognormal distribution. The bivariate PDF is expressed as follows [7]:

$$f\left(D, A \mid S_a = x\right) = \frac{1}{2\pi DA\sigma_{D|x}\sigma_{A|x}\left(1-\rho^2\right)^{1/2}} * \left\{\exp -\frac{1}{2\left(1-\rho^2\right)} * \left[\left(\frac{\ln D - \mu_{D|x}}{\sigma_{D|x}}\right)^2 + \left(\frac{\ln A - \mu_{A|x}}{\sigma_{A|x}}\right)^2 - 2\rho\left(\frac{\ln D - \mu_{D|x}}{\sigma_{D|x}}\right)\left(\frac{\ln A - \mu_{A|x}}{\sigma_{A|x}}\right)\right]\right\} \tag{11}$$

where $\mu_{D|x}$ and $\sigma_{D|x}$ are log-mean and log-standard deviation of the maximum interstory drift, respectively; $\mu_{A|x}$ and $\sigma_{A|x}$ are log-mean and the log-standard deviation of the acceleration, respectively; ρ is the correlation coefficient between $\ln D$ and $\ln A$.

The mean vector μ^{T} and covariance Σ of the bivariate PDF are expressed as follows:

$$\boldsymbol{\mu}_{\mathbf{D},\mathbf{A}}^{\mathrm{T}} = \left[\mu_{D|x}, \mu_{A|x}\right] \qquad \boldsymbol{\Sigma} = \begin{bmatrix} \sigma_{D|x}^2 & \rho\sigma_{D|x}\sigma_{A|x} \\ \rho\sigma_{D|x}\sigma_{A|x} & \sigma_{A|x}^2 \end{bmatrix} \tag{12}$$

ρ can be estimated by the following expression:

$$\widehat{\rho} = \frac{(1/n)\sum_{i=1}^{n}\left[\left(\ln D_i\right)\cdot\left(\ln A_i\right)\right] - \widehat{\mu}_{D|im}\cdot\widehat{\mu}_{A|im}}{\widehat{\sigma}_{D|im}\cdot\widehat{\sigma}_{A|im}} \tag{13}$$

where $\widehat{\rho}$ is the estimator of the correlation coefficient ρ; n is the number of ground inputs; $\widehat{\mu}_{D|im}$ and $\widehat{\sigma}_{D|im}$ are the estimators of log-mean and log-standard deviation of the maximum interstory drift, respectively; $\widehat{\mu}_{A|im}$ and $\widehat{\sigma}_{A|im}$ are the estimators of log-mean and log-standard deviation of acceleration, respectively.

3. Two-Dimensional Performance Limit State Function

3.1. Performance Function of Both Limit States. The performance function of both limit states, which allows considering the relationship between EDPs and limit thresholds, is defined as follows [7, 60]:

$$G\left(\left(\boldsymbol{\Delta}_{(\mu_\Delta,\sigma_\Delta)}, \mathbf{Z}_{(\mu_\mathbf{Z},\sigma_\mathbf{Z})}\right), (\mathbf{D}, \mathbf{A})\right) = \left(\frac{\mathbf{A}}{\mathbf{Z}_{(\mu_\mathbf{Z},\sigma_\mathbf{Z})}}\right)^{N_1} + \left(\frac{\mathbf{D}}{\boldsymbol{\Delta}_{(\mu_\mathbf{Z},\sigma_\mathbf{Z})}}\right)^{N_2} - 1 \tag{14}$$

where $\mathbf{D}$ is the vector of the maximum interstory drift, $\boldsymbol{\Delta}$ is the vector of the maximum interstory drift threshold, $\mathbf{A}$ is the vector of the acceleration, $\mathbf{Z}$ is the vector of the acceleration threshold, μ_Δ and σ_Δ are mean and standard deviation of the interstory drift threshold, respectively, and $\mu_\mathbf{Z}$ and $\sigma_\mathbf{Z}$ are mean and standard deviation of the acceleration threshold, respectively. $\mathbf{D}$ and $\mathbf{A}$ are considered as random variables and follow the bivariate lognormal distribution. $\boldsymbol{\Delta}$ and $\mathbf{Z}$ are assumed to be lognormally distributed. μ_Δ and $\mu_\mathbf{Z}$ are described by the IMP variables.

The desired performance function can guarantee that the two peak EDPs stay below their respective critical values over a specified duration. When $N_1 = 1$, a sector/triangle acceptable region is generated to realize the equivalent between the notion of the performance function and treatment of joint probability density function (JPDF) of the two dependent EDPs. Therefore, (14) can be simplified as

$$G\left(\left(\boldsymbol{\Delta}_{(\mu_\Delta,\sigma_\Delta)}, \mathbf{Z}_{(\mu_\mathbf{Z},\sigma_\mathbf{Z})}\right), (\mathbf{D}, \mathbf{A})\right) = \left(\frac{\mathbf{A}}{\mathbf{Z}_{(\mu_\mathbf{Z},\sigma_\mathbf{Z})}}\right) + \left(\frac{\mathbf{D}}{\boldsymbol{\Delta}_{(\mu_\Delta,\sigma_\Delta)}}\right)^{N_2} - 1 \tag{15}$$

When the simplest case with $N_2 = 1$ is considered, the performance function is written as

$$G\left(\left(\boldsymbol{\Delta}_{(\mu_\Delta,\sigma_\Delta)}, \mathbf{Z}_{(\mu_\mathbf{Z},\sigma_\mathbf{Z})}\right), (\mathbf{D}, \mathbf{A})\right) = \frac{\mathbf{D}\mathbf{Z}_{(\mu_\mathbf{Z},\sigma_\mathbf{Z})} + \mathbf{A}\boldsymbol{\Delta}_{(\mu_\Delta,\sigma_\Delta)}}{\boldsymbol{\Delta}_{(\mu_\Delta,\sigma_\Delta)}\mathbf{Z}_{(\mu_\mathbf{Z},\sigma_\mathbf{Z})}} - 1 \tag{16}$$

3.2. The IMP Model. Recent work [49, 50] indicated that the MP model could deal with the problems where correlated variables and independent variables coexist. However, Ni et al. [52] and Jiang et al. [51] stated the main deficiencies of the existing MP model and then proposed an IMP model. The correlation coefficient between uncertain-but-bounded variables in the IMP model can be easily calculated and the uncertainty domain of the bounded variables can be explicitly expressed through a matrix inequality. When a two-dimensional problem with bounded variables μ_Δ and $\mu_\mathbf{Z}$ is considered, the IMP model degenerates into a parallelogram. The marginal intervals of the two variables μ_Δ and $\mu_\mathbf{Z}$ are denoted as μ_Δ^I and $\mu_\mathbf{Z}^I$, respectively. The two marginal intervals μ_Δ^I and $\mu_\mathbf{Z}^I$ are defined as

$$\mu_\Delta^I = \left[\mu_\Delta^L, \mu_\Delta^R\right], \qquad \mu_\Delta^C = \frac{\left(\mu_\Delta^L + \mu_\Delta^R\right)}{2}, \qquad \mu_\Delta^W = \frac{\left(\mu_\Delta^R - \mu_\Delta^L\right)}{2} \tag{17}$$

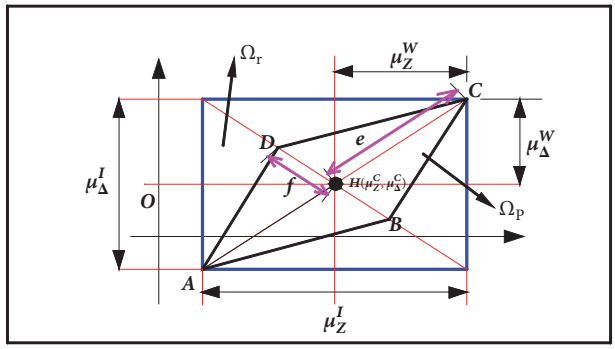

Figure 1: The IMP convex model with a two-dimensional problem.

$$\begin{aligned}\mu_{\mathbf{Z}}^{\boldsymbol{I}} &= \left[\mu_Z^L, \mu_Z^R\right],\\ \mu_Z^C &= \frac{\left(\mu_Z^L + \mu_Z^R\right)}{2},\\ \mu_Z^W &= \frac{\left(\mu_Z^R - \mu_Z^L\right)}{2}\end{aligned} \tag{18}$$

where μ_Δ^L and μ_Δ^R are the lower bound and upper bound of $\mu_\Delta^{\boldsymbol{I}}$; μ_Z^L and μ_Z^R are the lower bound and upper bound of $\mu_{\mathbf{Z}}^{\boldsymbol{I}}$; μ_Δ^C and μ_Z^C represent the midpoints of $\mu_\Delta^{\boldsymbol{I}}$ and $\mu_{\mathbf{Z}}^{\boldsymbol{I}}$; μ_Δ^W and μ_Z^W represent interval radii of the two marginal intervals. If bounded variables μ_Δ and $\mu_{\mathbf{Z}}$ are independent of each other, the uncertainty domain of the two variables will become a rectangular domain $[\mu_\Delta^L, \mu_\Delta^R] \times [\mu_Z^L, \mu_Z^R]$, expressed as Ω_r. If the two bounded variables are dependent, the uncertainty domain will form a parallelogram domain Ω_p, as shown in Figure 1. According to the principles proposed by Ni et al. [52], the uncertainty domain in the IMP model can be constructed.

It can be observed from Figure 1 that the center of the parallelogram coincides with that of the rectangular domain. Moreover, the shape of the parallelogram can exhibit the degree of correlation between $\mu_\Delta^{\boldsymbol{I}}$ and $\mu_{\mathbf{Z}}^{\boldsymbol{I}}$ (Ni et al. [52] have completed the proof). In the IMP model, a quadrilateral side need not be set to be parallel to the abscissa axis. From Figure 1, it can be seen that f represents the semi-axis length in the direction $\overrightarrow{HD}$ and e represents the semi-axis length in the direction $\overrightarrow{HC}$. A new correlation coefficient between uncertain-but-bounded variables can be defined as

$$\rho_{\Delta\mathbf{Z}} = \frac{e - f}{e + f} \tag{19}$$

where $\rho_{\Delta\mathbf{Z}}$ has the range $[-1\ 1]$, $\rho_{\Delta\mathbf{Z}} = \rho_{\mathbf{Z}\Delta}$ and $\rho_{\Delta\Delta} = \rho_{\mathbf{Z}\mathbf{Z}} = 1$. When $m = 0$ and $\rho_{\Delta\mathbf{Z}} = 1$, the bounded variables μ_Δ and $\mu_{\mathbf{Z}}$ are linearly and positively dependent. When $e = 0$ and $\rho_{\Delta\mathbf{Z}} = -1$, the two bounded variables are linearly and negatively dependent. When $e = f$ and $\rho_{\Delta\mathbf{Z}} = 0$, the two bounded variables are independent. When $0 < f < e$ and $\rho_{\Delta\mathbf{Z}} > 0$, the two bounded variables are positively dependent. When $0 < e < f$ and $\rho_{\Delta\mathbf{Z}} < 0$, the two variables are negatively dependent. Then, the symmetrical correlation matrix $\boldsymbol{\rho}$ can be defined as

$$\boldsymbol{\rho} = \begin{bmatrix}\rho_{\Delta\Delta} & \rho_{\Delta\mathbf{Z}}\\ \rho_{\mathbf{Z}\Delta} & \rho_{\mathbf{Z}\mathbf{Z}}\end{bmatrix} = \begin{bmatrix}1 & \rho_{\Delta\mathbf{Z}}\\ \rho_{\mathbf{Z}\Delta} & 1\end{bmatrix} \tag{20}$$

Subsequently, the uncertainty domain established by the IMP model can be explicitly expressed by the following matrix inequality [51, 52]:

$$-\mathbf{e} \le \boldsymbol{\rho}^{-1}\mathbf{T}^{-1}\mathbf{R}^{-1}\left(\boldsymbol{\mu} - \boldsymbol{\mu}^{\mathbf{C}}\right) \le \mathbf{e} \tag{21}$$

where the diagonal matrices $\mathbf{T}$, $\mathbf{R}$ and the vectors $\mathbf{e}$, $\boldsymbol{\mu}$, $\boldsymbol{\mu}^{\mathbf{C}}$ are defined as

$$\begin{aligned}\mathbf{T} &= \operatorname{diag}\left(\mathrm{w}_1, \mathrm{w}_2\right), \quad \mathrm{w}_{\boldsymbol{i}} = \frac{1}{\sum_{j=1}^{2}\left|\boldsymbol{\rho}\left(i, j\right)\right|},\ i = 1, 2\\ \mathbf{R} &= \operatorname{diag}\left(\mu_\Delta^W, \mu_Z^W\right),\\ \mathbf{e} &= \begin{pmatrix}1 & 1\end{pmatrix}^{\mathbf{T}},\\ \boldsymbol{\mu} &= \begin{pmatrix}\mu_\Delta & \mu_Z\end{pmatrix}^{\mathbf{T}},\\ \boldsymbol{\mu}^{\mathbf{C}} &= \begin{pmatrix}\mu_\Delta^C & \mu_Z^C\end{pmatrix}^{\mathbf{T}}\end{aligned} \tag{22}$$

in which diag $(\mathrm{w}_1, \mathrm{w}_2)$ represents the diagonal elements w_1 and w_2 of the diagonal matrix and $\boldsymbol{\rho}(i, j)$ represents the element in the ith row and the jth column of the correlation matrix $\boldsymbol{\rho}$. Further, a *Shape Matrix* C can be defined as [51, 52]

$$\mathbf{C} = \mathbf{RT}\boldsymbol{\rho} \tag{23}$$

Equation (21) can be rewritten as follows:

$$\left|\mathbf{C}^{-1}\left(\boldsymbol{\mu} - \boldsymbol{\mu}^{\mathbf{C}}\right)\right| \le \mathbf{e} \tag{24}$$

Note that when the interval radius $\mu_\Delta^{\boldsymbol{W}}$ is equal to μ_Z^W, the parallelogram is a rhomb. The IMP domain can be expressed as

$$\Omega_p = \left\{\boldsymbol{\mu} \mid \left|\mathbf{C}^{-1}\left(\boldsymbol{\mu} - \boldsymbol{\mu}^{\mathbf{C}}\right)\right| \le \mathbf{e}\right\} \tag{25}$$

Consider a general n-dimensional problem with marginal intervals $\mu_{\boldsymbol{i}}^{\boldsymbol{I}}$, $i = 1, 2, \cdots, n$, of uncertain variables. In such circumstances, the uncertain domain is a multidimensional parallelepiped. Analogous to the definition of (20), the correlation between any two uncertain-but-bounded variables μ_i and μ_j can be expressed by the correlation coefficient ρ_{ij}. Then, the correlation matrix $\boldsymbol{\rho}$ for all of bounded variables can be defined as [51, 52]

$$\boldsymbol{\rho} = \begin{bmatrix}1 & \rho_{12} & \cdots & \rho_{1n}\\ \rho_{21} & 1 & \cdots & \rho_{2n}\\ \cdots & \cdots & \ddots & \vdots\\ \rho_{n1} & \rho_{n2} & \cdots & 1\end{bmatrix} \tag{26}$$

where $\boldsymbol{\rho}$ is an $m \times m$ symmetric matrix. The analytical expression of the multidimensional parallelepiped uncertain domain can be derived in the similar way from the two-dimensional case, and the detailed process is omitted.

Remark 2. (i) When creating a new IMP model, we need the marginal intervals of all bounded variables and the correlation between any two variables. Assume that there are n-dimensional uncertain variables μ_i, i=1,2,...,n, and m test samples $\boldsymbol{\mu}^{(r)}$, r=1,2,...,m, then the detailed procedure of building the IMP convex model could be found in Jiang et al. [49, 50] and Ni et al. [52]. For multidimensional problems, the IMP model can be efficiently developed through decomposing the complicated n-dimensional problems into $n(n+1)/2$ sample two-dimensional problems.

3.3. Normalization of the Uncertainty Domain Ω_p. To transform the IMP model into a regular interval (bounded) model, a regularization method will be performed in this section. Then, the parallelepiped uncertainty domain Ω_p can become a multidimensional cube after the regularization method is adopted. Introduce the following transformation:

$$\boldsymbol{\delta} = \mathbf{C}^{-1}\left(\boldsymbol{\mu} - \boldsymbol{\mu}^{\mathbf{C}}\right) \tag{27}$$

The uncertain-but-bounded variables $\boldsymbol{\mu}$ can be mapped into the $\boldsymbol{\delta}$ space and then the uncertainty domain Ω_p becomes an n-dimensional cube Ω^*, denoted as

$$\Omega^* = \{\boldsymbol{\delta} \mid |\boldsymbol{\delta}| \le \mathbf{e}\} \tag{28}$$

where $\boldsymbol{\delta} = \{\delta_1, \delta_2, \ldots, \delta_n\}$.

The semi-axis length e and f can be solved when only translation, scaling, and rotation are required in the above process. Thus, this regularization method can be categorized as affine transformation proposed by Jiang et al. [49, 51]. By using the transformation, the uncertainty domain Ω_p becomes a standard cube center and the length of each side is 2 in $\boldsymbol{\delta}$ space. Meanwhile, the bounded variables are independent of each other in $\boldsymbol{\delta}$ space.

4. Application to Reliability Analysis

The performance limit state equation (15) defines the failure mode of the RC structure and it plays an important role in the reliability assessment. For convenience of expression, the vectors **D**, **A**, **Δ**, **Z** are uniformly expressed as **X**={**D, A, Δ, Z**}. Through the regularization of the uncertain variables **X** and $\boldsymbol{\mu}$ into **u** and $\boldsymbol{\delta}$ elaborated in Section 3, the limit state function $G(\mathbf{X}, \boldsymbol{\mu})$ can be mapped into the regularized limit state function $G(\mathbf{u}, \boldsymbol{\delta})$. Since the random and bounded variables coexist, correspondingly, the limit state $G(\mathbf{u}, \boldsymbol{\delta})$ constitutes a cluster of limit state surfaces in the standard **u** space. In the whole **u**-space $\Omega_{\mathbf{u}}$, a safe region of the **limit state function $G(\mathbf{u}, \boldsymbol{\delta})$** is denoted as $\Omega_s = \{\mathbf{u} \mid \min_{\boldsymbol{\delta}} G(\mathbf{u}, \boldsymbol{\delta}) < 0\}$ and a critical region is expressed as $\Omega_c = \{\mathbf{u} \mid G(\mathbf{u}, \boldsymbol{\delta}) = 0\}$. Then a failure region can be denoted as $\Omega_f = \Omega \setminus (\Omega_s \cup \Omega_c)$. Therefore, the failure probability with both random and bounded variables can be defined as

$$P_f^U = \Pr\left\{\mathrm{M}(\mathbf{u}) = \min_{\boldsymbol{\delta}} G(\mathbf{u}, \boldsymbol{\delta}) > 0 \mid \boldsymbol{\delta} \in \Omega^*\right\} \tag{29}$$

where $\mathrm{M}(\mathbf{u})$ is the minimization of the limit state function and can be solved by the following optimization problem:

$$\begin{aligned} \min_{\boldsymbol{\delta}} \quad & G(\mathbf{u}, \boldsymbol{\delta}) \\ \text{s.t.} \quad & |\boldsymbol{\delta}| \le \mathbf{e} \end{aligned} \tag{30}$$

In this paper, a global optimization algorithm called as DIRECT algorithm [61] is used to realize the global optimum. Then, (8) can be rewritten as

$$\begin{aligned} \lambda = \int & \Pr\left\{\mathrm{M}(\mathbf{u}) = \min_{\boldsymbol{\delta}} G(\mathbf{u}, \boldsymbol{\delta}) > 0 \mid \boldsymbol{\delta} \in \Omega^*\right\} \\ & \cdot \left|h_{S_a}(x)\right| |\mathrm{d}(x)| \end{aligned} \tag{31}$$

Note that the failure probabilities in 50 years can be obtained by substituting (31) into (5).

If the FORM method is used to solve (29), (29) can be obtained by using the following double-loop optimization:

$$\begin{aligned} \beta^* = \min_{\mathbf{u}} \quad & \mathbf{u}^{\mathbf{T}}\mathbf{u} \\ \text{s.t.} \quad & \min_{\boldsymbol{\delta}} G(\mathbf{u}, \boldsymbol{\delta}) = 0 \\ & |\boldsymbol{\delta}| \le \mathbf{e} \end{aligned} \tag{32}$$

where β^* is the minimum reliability index. A mathematical programming method (MPM) and a single-loop iterative (SLI) method [35] were proposed to solve the above double-loop optimization problem. Subsequently, the maximum failure probability of a structure can be approximately calculated by the following expression:

$$P_f^U = \Phi(-\beta^*) = 1 - \int_{-\infty}^{\beta^*} \frac{1}{\sqrt{2\pi}} \exp\left(-\frac{u^2}{2}\right) \mathrm{d}u \tag{33}$$

Geometrically, β^* is the shortest distance from the origin to the region Ω_c in the standard **u**-space Ω. Some literatures [38, 62, 63] showed that the reliability of a structure with both random and convex variables could be evaluated using the minimum reliability index. However, β^* could not accurately measure the reliability of a structure when the performance function was nonlinear or had multiple design points [64, 65]. Therefore, an efficient method based on active learning Kriging model (ALK) will be used to predict (30).

5. ALK-MGHAR for the Reliability Analysis

5.1. Fundamental Theory. To reduce the computational cost, an ALK method [43, 47, 48, 66–68] is introduced to approximate the performance in the region of interest rather than throughout the overall space. Based on the Kriging model, then, the failure probability P_f^U can be calculated through MCS method. When the Kriging model is built, the performance function need not be approximated throughout the whole uncertainty space, but only in the region of interest. An imitated Efficient Global Optimization (EGO) for global optimization is usually required in ALK models. When searching

the minimum value within global optimization, we require selecting the points at which the value of the objective function $G(\mathbf{u}, \boldsymbol{\delta})$ has the maximum expectation value to be smaller than the current least value. Therefore, a learning function called Expected Improvement Function (EIF) proposed by Jones et al. [69] was employed in EGO. For the problems with both random and bounded variables, a right predication for the sign of the objective function $G(\mathbf{u}, \boldsymbol{\delta})$ rather than the specific value of $G(\mathbf{u}, \boldsymbol{\delta})$ can be adopted in the Kriging model. In order to greatly enhance the prediction for the sign of $G(\mathbf{u}, \boldsymbol{\delta})$, the point at which the sign of $G(\mathbf{u}, \boldsymbol{\delta})$ has the maximum risk value to be wrongly predicted should be added into the DoE. Moreover, an active learning function termed as Expected Risk Function (ERF) [43, 44] is used to recognize this point. The reason why a Kriging model providing a right prediction for the sign of $G(\mathbf{u}, \boldsymbol{\delta})$ can satisfy the precision requirement of MGHAR is given by the following corollary. Note that the proposed corollary is based on the existing properties [45, 64]. Therefore, the proof of the corollary is omitted.

Corollary 3. *If a Kriging model can rightly predict the sign of* $G(\mathbf{u}, \boldsymbol{\delta})$*, then the sign of* $\min_{\boldsymbol{\delta}} G(\mathbf{u}, \boldsymbol{\delta})$ *is the same as that of* $\min_{\boldsymbol{\delta}} \widehat{G}(\mathbf{u}, \boldsymbol{\delta})$*. Sequentially, the optimization problem defined by (30) can be replaced by the following optimization:*

$$\begin{aligned} \min_{\boldsymbol{\delta}} \quad & \widehat{G}(\mathbf{u}, \boldsymbol{\delta}) \\ \text{s.t.} \quad & |\boldsymbol{\delta}| \le \mathbf{e} \end{aligned} \tag{34}$$

5.2. Revisiting Kriging Model. For the sake of convenience, we use the vector $\boldsymbol{\Theta}$ to replace $(\mathbf{A}, \mathbf{D}, \mathbf{Z}, \boldsymbol{\Delta})$. The Kriging model $\mathbf{G}(\boldsymbol{\Theta})$ can be denoted as

$$\mathbf{G}(\boldsymbol{\Theta}) = F(\boldsymbol{\Theta}, \boldsymbol{\beta}) + z(\boldsymbol{\Theta}) \tag{35}$$

where $F(\boldsymbol{\Theta}, \boldsymbol{\beta})$ is the polynomial regression part and $\boldsymbol{\beta}$ is the vector of regression coefficients. $z(\boldsymbol{\Theta})$ is a Gaussian random process whose mean and covariance are expressed as

$$\begin{aligned} E[z(\boldsymbol{\Theta})] &= 0 \\ \operatorname{cov}[z(\mathbf{a}), z(\mathbf{b})] &= \sigma^2 [\Re(\boldsymbol{\theta}, \mathbf{a}, \mathbf{b})] \end{aligned} \tag{36}$$

where σ is the standard deviation of the Gaussian process, $\mathbf{a}$ and $\mathbf{b}$ are two arbitrary points, and $\Re(\cdot)$ is a correlation function with parameters $\boldsymbol{\theta}$, $\mathbf{a}$, and $\mathbf{b}$. Here, the Gaussian function is selected and it can be expressed as

$$\Re(\boldsymbol{\theta}, \boldsymbol{c}, \boldsymbol{d}) = \exp\left[-\sum_{i=1}^{n} \theta_i (c_i - d_i)^2\right] \tag{37}$$

where n is the number of sample points and θ_i, c_i, and d_i are the ith component of $\boldsymbol{\theta}$, $\boldsymbol{c}$, and $\boldsymbol{d}$, respectively.

The Kriging model needs a DoE to define its statistical parameters and then predictions for $G(\boldsymbol{\Theta})$ at unknown points can be implemented. Given a DoE: $[\boldsymbol{\Theta}^{(1)}, \boldsymbol{\Theta}^{(2)}, \cdots, \boldsymbol{\Theta}^{(m)}]^T$ with $\boldsymbol{\Theta}^{(i)}$ the ith training points and a vector of the performance function $\boldsymbol{G} = [\boldsymbol{G}(\boldsymbol{\Theta}^{(1)}), \boldsymbol{G}(\boldsymbol{\Theta}^{(2)}), \cdots, \boldsymbol{G}(\boldsymbol{\Theta}^{(m)})]^T$ with $\boldsymbol{G}(\boldsymbol{\Theta}^{(i)})$ the ith function value. In this study, ordinary Kriging model [70] is utilized to simplify (35) which means that $F(\boldsymbol{\Theta}, \boldsymbol{\beta})$ can be replaced by a constant $\widehat{\beta}$. Therefore, the predicted value $\widehat{G}(\boldsymbol{\Theta})$ and the predicted variance $s^2(\boldsymbol{\Theta})$ are, respectively, represented by

$$\widehat{G}(\boldsymbol{\Theta}) = \widehat{\beta} + \mathbf{r}^T(\boldsymbol{\Theta}) \mathbf{R} \left(G - \mathbf{1}\widehat{\beta}\right) \tag{38}$$

$$s^2(\boldsymbol{\Theta}) = \sigma^2 \left[1 - \boldsymbol{r}^T(\boldsymbol{\Theta}) \mathbf{R} \boldsymbol{r}(\boldsymbol{\Theta}) + \frac{\left(1 - \mathbf{1}^T \mathbf{R}^{-1} \boldsymbol{r}(\boldsymbol{\Theta})\right)^2}{\mathbf{1}^T \mathbf{R}^{-1} \mathbf{1}}\right] \tag{39}$$

In (38)-(39),

$$\widehat{\beta} = \left(\mathbf{1}^T \mathbf{R}^{-1} \mathbf{1}\right)^{-1} \mathbf{1}^T \mathbf{R}^{-1} G \tag{40}$$

$$\sigma^2 = \frac{1}{m} \left(G - \widehat{\beta}\mathbf{1}\right)^T \mathbf{R}^{-1} \left(G - \widehat{\beta}\mathbf{1}\right) \tag{41}$$

$$\boldsymbol{r}(\boldsymbol{\Theta}) = \left[\Re\left(\boldsymbol{\theta}, \boldsymbol{\Theta}, \boldsymbol{\Theta}^{(1)}\right), \Re\left(\boldsymbol{\theta}, \boldsymbol{\Theta}, \boldsymbol{\Theta}^{(2)}\right), \cdots \Re\left(\boldsymbol{\theta}, \boldsymbol{\Theta}, \boldsymbol{\Theta}^{(m)}\right)\right] \tag{42}$$

In (38)-(39), $\mathbf{R}$ is an $m \times m$ matrix whose element is given by

$$R_{ij} = \Re\left(\boldsymbol{\theta}, \boldsymbol{\Theta}^{(i)}, \boldsymbol{\Theta}^{(j)}\right) \tag{43}$$

In (38)-(42), $\mathbf{1}$ denotes m-dimensional unit vector and $\boldsymbol{r}(\boldsymbol{\Theta})$ is the correlation vector between $\boldsymbol{\Theta}$ and ith training point.

The parameter $\boldsymbol{\theta}$ in (42)-(43) can be solved through the unconstrained optimization problem, expressed as

$$\boldsymbol{\theta}^{\text{opt}} = \arg \min_{\theta} \left(|\mathbf{R}|^{1/m} \sigma^2\right) \tag{44}$$

Because only the Kriging model with the global optimum parameter $\boldsymbol{\theta}^{\text{opt}}$ can provide the most exact predictions for the performance function $G(\boldsymbol{\Theta})$, the optimal parameter $\boldsymbol{\theta}^{\text{opt}}$ should be solved through global optimization strategy and the modified DIRECT algorithm [71] is adopted in this paper.

The Kriging model provides a predicted value $\widehat{G}(\boldsymbol{\Theta})$ for the performance function $G(\boldsymbol{\Theta})$ at an unknown point $\boldsymbol{\Theta}$. Nevertheless, there exist some uncertainties in this prediction process because a Gaussian random variate $G(\boldsymbol{\Theta}) \sim N(\widehat{G}(\boldsymbol{\Theta}), s^2(\boldsymbol{\Theta}))$. It should be noted that $\widehat{G}(\boldsymbol{\Theta})$ is only an approximate value rather than an actual value of $G(\boldsymbol{\Theta})$. Therefore, there exists a risk that the sign of $G(\boldsymbol{\Theta})$ is wrongly predicted. To implement the prediction for the sign of $G(\boldsymbol{\Theta})$, the point at which the sign of $G(\boldsymbol{\Theta})$ has the largest risk value to be wrongly predicted needs to be identified. Then this point should be added into DoE and the sign prediction of $G(\boldsymbol{\Theta})$ is significantly improved. To identify the aforesaid point and build an ALK model, a learning function named ERF is

introduced to provide a precise sign prediction and it is expressed as

$$\begin{aligned} E\left[R\left(\boldsymbol{\Theta}\right)\right] &= -\operatorname{sign}\left(\widehat{G}\left(\boldsymbol{\Theta}\right)\right)\widehat{G}\left(\boldsymbol{\Theta}\right)\Phi\left(-\operatorname{sign}\left(\widehat{G}\left(\boldsymbol{\Theta}\right)\right)\frac{\widehat{G}\left(\boldsymbol{\Theta}\right)}{s\left(\boldsymbol{\Theta}\right)}\right) \\ &\quad + s\left(\boldsymbol{\Theta}\right)\phi\left(\frac{\widehat{G}\left(\boldsymbol{\Theta}\right)}{s\left(\boldsymbol{\Theta}\right)}\right) \end{aligned} \tag{45}$$

in which sign(·) is the sign function and $\Phi(\cdot)$ and $\phi(\cdot)$ are the cumulative distribution function (CDF) and the PDF of the standard normal distribution, respectively. If a point is able to maximize ERF, the sign of $G(\boldsymbol{\Theta})$ at this point will have the largest risk being wrongly predicted. Subsequently, this point is added into DoE. The procedure of combining MCS and ALK-MGHAR named ALK-MGHAR-MCS will be presented in Section 5.3.

5.3. Summary of ALK-MGHAR-MCS for Reliability Analysis

Step 1 (selection of recorded ground motions). Thirty real earthquake records (M=6.0-7.0, R=15-20km) are chosen whose response shapes are similar to the shape of the target response spectrum, according to the selection of ground motion inputs elaborated by Liu et al. [7].

Step 2 (analysis of the structure subjected to each of the ground motions). Analyze a given structure under each of the ground motions generated in Step 1 which is scaled from low hazard levels to higher hazard levels until a structural collapse occurs. The maximum interstory drift can be obtained using IDA and the maximum acceleration needs to be calculated through NHA. The present writer [7] illustrated the methodology of calculating the two EDPs.

Step 3 (estimate of the mean and the standard deviation originated from (11)). The mean and the standard deviation from the response samples obtained in Step 2 are required and then the bivariate PDF can be evaluated. Subsequently, a great deal of sampling points in the performance function (11) can be generated through the bivariate PDF.

Step 4 (define the initial DoE). (a) The number of training points included in the initial DOE is supposed to be small. The number of 12 is selected in this study, according to the existing investigations [47, 48].

(b) Latin hypercube sampling (LHS) is utilized to produce the samples, which are uniformly distributed in the uncertain space. For bivariate lognormal variables $\mathbf{D}$ and $\mathbf{A}$, Nataf transformation is used to transform the two variables into the approximately equivalent normal variables. The lower and upper bounds of equivalent normal variables are chosen as $F_i^{-1}(\Phi(\pm 5))$ and then these variables are converted into the standard $\mathbf{u}$-space. Here, $F_i^{-1}(\cdot)$ is the inverse CDF of equivalent normal variables. Two steps are required for the IMP convex variables $\mu_{\boldsymbol{\Delta}}$ and $\mu_{\mathbf{Z}}$. Firstly, the IMP model needs to be constructed. Then LHS is used to generate a large amount of samples uniformly covering the space defined by (28) which is mapped into the original space defined in (25).

(c) These chosen sampling points are used to estimate the performance function $G(\boldsymbol{\Theta})$ and then an initial Kriging model is constructed with the initial DoE.

Step 5 (generate a large amount of samples as candidate points). (a) Denote the set of candidate points as $\boldsymbol{\Omega}_{\mathrm{LHS}}$. For bivariate lognormal random variables, MCS is adopted to generate samples. For IMP convex variables, LHS is employed to obtain the uniformly distributed sampling points as Step 4.

(b) Denote the number of sampling points in $\boldsymbol{\Omega}_{\mathrm{LHS}}$ as $N_{\Omega_{\mathrm{LHS}}}$. To cover the overall uncertain space, the number of points $N_{\Omega_{\mathrm{LHS}}}$ ($N_{\Omega_{\mathrm{LHS}}} = 10^5$) is supposed to be sufficiently large. Note that the performance function is not calculated in this stage. All of the points are only considered as candidate points. The newly increased training points in the next few steps will be chosen among the points.

Step 6 (identify the newly added training points in the set of the candidate points). The point maximizing ERF among the candidates is selected as a new training point, which should be added into the DoE. The point is expressed as $(\mathbf{X}^{(*)}, \boldsymbol{\mu}^{(*)})$.

Step 7 (stopping condition). When the maximum value of ERF is small enough, the sign of the performance function $G(\mathbf{X}, \boldsymbol{\mu})$ in the uncertain space has little risk value to be wrongly predicted. Then, go to Step 9. The stopping condition adopted here is $E[R(\mathbf{X}^{(*)}, \boldsymbol{\mu}^{(*)})] \leq 10^{-4}$.

Step 8 (obtain an updated DoE and construct a new Kriging model). If the stopping condition in Step 7 is not satisfied, $G(\mathbf{X}, \boldsymbol{\mu})$ at the point $(\mathbf{X}^{(*)}, \boldsymbol{\mu}^{(*)})$ should be calculated. Add the point $(\mathbf{X}^{(*)}, \boldsymbol{\mu}^{(*)})$ into the DoE and construct a new Kriging model. Go back to Step 6.

Step 9. Implement MGHAR with MCS presented in Section 2 based on the Kriging model.

6. Case Study: A Six-Story RC Building

6.1. Design of the Case Study according to Chinese Codes. To verify the efficiency and accuracy of the proposed method, a sample six-story reinforced concrete (RC) frame building is taken for case study in this paper. The example structure is designed according to Chinese codes [72], which represents the typical mid-rise RC buildings in China. The geographical location of the modelled building is designated to be western China. This is a Class II site, with eight times the intensity of an earthquake and the designing ground acceleration is set as 0.20. The seismic grade of the example building is level 2 [73]. The plane and elevation views of the designed frame structure are shown in Figure 2. The total height of building is 19.8 m. The lengths of longitudinal spans and transversal spans are 36 m and 14.4 m, respectively. The columns and beams' cross sections are 600 mm×600 mm and 300 mm×500 mm, respectively. The distributed steel in beams and columns is designed by using Chinese codes [72], as shown in Figure 3.

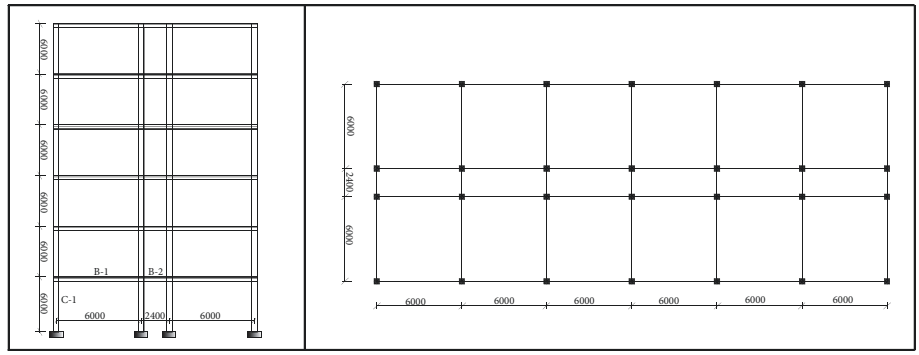

Figure 2: The plane and elevation views of the designed frame structure.

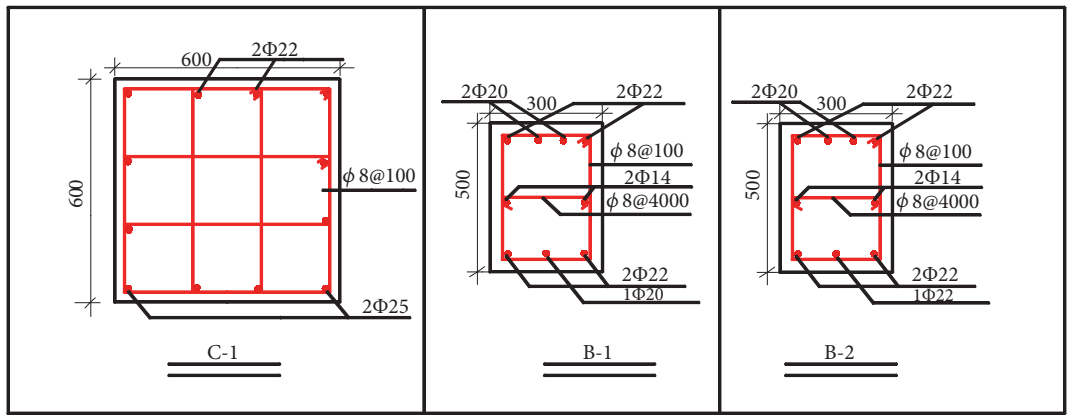

Figure 3: The distributed steel in columns and beams.

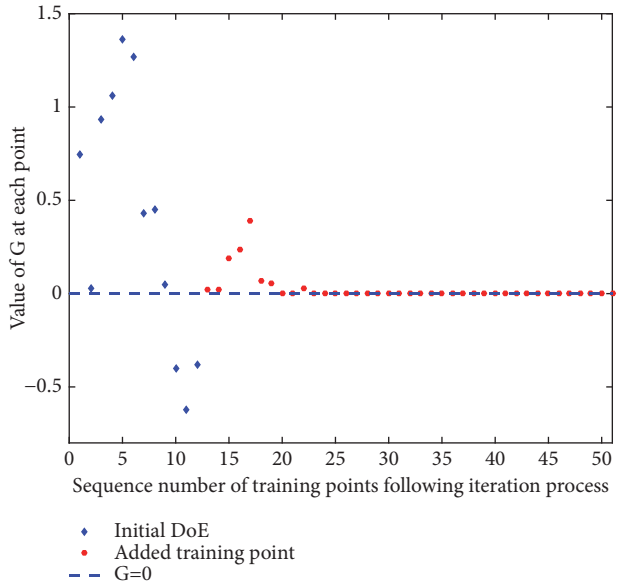

Figure 4: DoE obtained by ALK-MGHAR.

6.2. Modeling of the Designed RC Building. By using the finite element platform OpenSees [74], a three-dimensional model of the given structure (Figure 4) can be developed in this section. A rigid diaphragm MPC (multipoint constraints) is employed to model the floor concrete slabs. Nonlinear beam-column elements are used to model column and beam members. The Kent-Scott-Park model with no tension stiffening is adopted to model the concrete material. Column and beam cross sections are discretized to fibers of confined concrete, unconfined concrete, and steel reinforcement. The structure is considered as deterministic and other parameters are not regarded as uncertain in the present analysis. The parameters for confined concrete (identified by the subscript "core") are listed as $f_{c,core}$ =34.5MPa, $f_{u,core}$ =24.1MPa, $\varepsilon_{0,\text{core}}$ =0.005, $\varepsilon_{\text{u,core}}$ =0.020. The parameters for unconfined concrete (identified by the subscript "cover") are described as follows: $f_{c,cover}$=27.6MPa, $f_{u,cover}$=0MPa, $\varepsilon_{0,\text{cover}}$=0.002, $\varepsilon_{\text{u,cover}}$=0.006. A bilinear material called Steel01 material is used to model the reinforcing steel with parameters E=206GPa, f_{y}=400MPa, and b=0.01. The structural responses such as interstory drift and acceleration can be, respectively, obtained through IDA and NHA. The fundamental mode for the given RC structure is set at 1.0018 sec by modal analysis.

6.3. Determination of Performance Limit Levels and the Uncertainty Domain. In this study, structural performance limit states are partitioned into four levels, i.e., normal operation (NO), immediate occupancy (IO), life safety (LS), and collapse prevention (CP). Limit states of the interstory drift and

the acceleration are simultaneously considered in this study. The threshold values of both EDPs under each performance level are described as random variables, listed in Table 1. The median of random variables under each performance level is treated as the IMP variables. The marginal intervals of the uncertain-but-bounded variables are shown in Table 2. The correlation coefficients between the bounded variables defined by (19) are $\rho_{\Delta Z} = \rho_{Z\Delta} = 0.33$. The correlation matrices under four performance levels can be expressed as $\boldsymbol{\rho}_{\mathrm{NO}}$, $\boldsymbol{\rho}_{\mathrm{IO}}$, $\boldsymbol{\rho}_{\mathrm{LS}}$, and $\boldsymbol{\rho}_{\mathrm{CP}}$. Then all of the correlation matrices can be built:

$$\boldsymbol{\rho}_{\mathrm{NO}} = \boldsymbol{\rho}_{\mathrm{IO}} = \boldsymbol{\rho}_{\mathrm{LS}} = \boldsymbol{\rho}_{\mathrm{CP}} = \begin{bmatrix} 1 & 0.33 \\ 0.33 & 1 \end{bmatrix} \tag{46}$$

According to (22), the uncertainty domain Ω_{p} can be explicitly expressed as

$$\begin{aligned} &\Omega_{\mathrm{p}} \\ &= \left\{ \boldsymbol{\mu} \left| \begin{bmatrix} 0.0029 & -0.4670 \\ -0.0009 & 1.4788 \end{bmatrix} \begin{pmatrix} \mu_{\Delta} - \mu_{\Delta}^{C} \\ \mu_{Z} - \mu_{Z}^{C} \end{pmatrix} \left| \left(\boldsymbol{\mu} - \boldsymbol{\mu}^{\mathrm{C}} \right) \right| \right. \right. \\ &\left. \left. \leq \begin{pmatrix} 1 \\ 1 \\ 1 \end{pmatrix} \right\} \end{aligned} \tag{47}$$

Then, the IMP model is transformed into the standard $\boldsymbol{\delta}$-space. Equation (14) will be a highly nonlinear performance function in the random space if $N_1 \geq 2$ and/or $N_2 \geq 2$.

7. Discussion

7.1. Reliability Analysis with Performance Function (16)

7.1.1. Application of ALK-MGHAR to Performance Function (16). Before performing ALK-MGHAR, the ground motion hazard analysis defined by (4) needs to be investigated. Since the site conditions defined in Section 6.1 are known, the two unknown parameters k_0 and k in (4) are calculated through the interpolation method. Here, $k_0 = 7.9203 \times 10^{-5}$ and $k = 2.3814$. After the maximum seismic failure probability is estimated by ALK-MGHAR, the failure probability for different limit states in 50 years can be obtained by combining the calculated seismic failure probability with ground motion hazard curve. A Kriging model should be constructed to have a right prediction for the sign of the performance function $G(\boldsymbol{\Theta})$. Based on the procedure elaborated in Section 5.3, 12 training points are chosen to build an initial Kriging model and then the iterative process begins. After 51 iterations, the stopping condition is satisfied and 51 training points are totally added into DoE. Moreover, the Kriging model is updated for 51 times. Taking CP performance level as an example, the DoE including initial and added training points obtained by ALK-MGHAR is depicted in Figure 4. It can be observed that a plenty of the added training points focus on the vicinity of the limit state $G(\mathbf{X}, \boldsymbol{\mu}) = 0$. This demonstrates that ALK-MGHAR is found capable of only locally approximating the performance function in the region of interest rather than in the overall uncertain space.

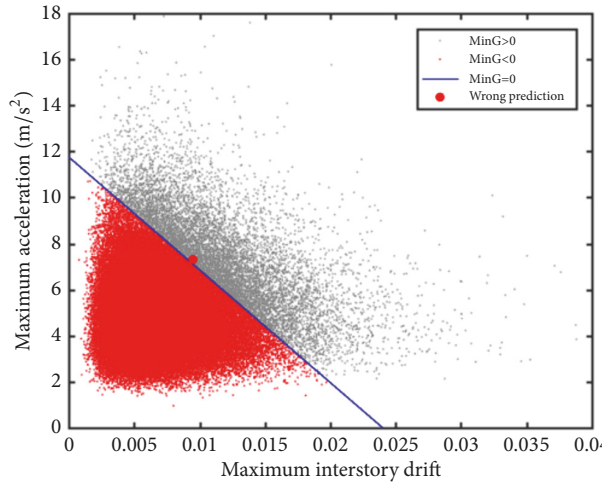

FIGURE 5: Sign of the minimum performance function with N_2=1 predicted by ALK-MGHAR.

After the Kriging model is built, the optimization problem (30) can be replaced by the optimization (34). This means that there exists a risk that the sign of the actual performance function is wrongly predicted. Then MCS can be carried out based on the Kriging model. 10^5 sampling points are used and the global optimization algorithm is utilized to search the minimum value of the Kriging model at each simulated sample. The sign of the minimal function value at each sample is predicted through ALK-MGHAR, as shown in Figure 5. It can be seen that only one sign is wrongly predicted. This indicates the accuracy of the proposed method.

7.1.2. Different Methods for Reliability Analysis. When the performance function (16) is adopted in this subsection, the maximum failure probability defined by (7) can be calculated using different numerical methods, such as MCS, MPM, SLI, and the proposed ALK-MGHAR. Then the failure probabilities under different performance levels in 50 years can be obtained by substituting (9) into (5). Note that MPM and SLI originated from Luo et al. [35] are generally employed to solve a double-loop optimization problem. Therefore, both MPM and SLI based on FORM can be used to solve the optimization problem (2). The failure probabilities in 50 years obtained by different methods are shown in Table 3. It can be observed that both MPM and SLI yield the satisfactory results. This is because the performance function (16) is linear at this moment. Therefore, the accuracy of MPM and SLI has been less affected. Moreover, the computation cost of ALK-MGHAR is much less than that of other different methods. For example, MCS requires $2 \times 100 \times 10^5$ function computations whereas the advocated method only requires 63 calls to the performance function. However, it is also found that the computational results obtained by the proposed method are in good coincidence with those obtained by MCS. These findings illustrate the efficiency and accuracy of ALK-MGHAR.

Table 1: Threshold capacity values of interstory drift and peak floor acceleration.

Threshold capacities of both the EDPs	NO level		IO level		LS level		CP level	
	Mean	SD[1]	Mean	SD[1]	Mean	SD[1]	Mean	SD[1]
Interstory drift threshold	$\mu_{\Delta 1}$	0.002	$\mu_{\Delta 2}$	0.005	$\mu_{\Delta 3}$	0.015	$\mu_{\Delta 4}$	0.025
Acceleration threshold	μ_{Z1}	0.4	μ_{Z2}	0.6	μ_{Z3}	0.8	μ_{Z4}	1.2

1: standard deviation of the interstory drift threshold and acceleration originated from Sun et al. [53].

Table 2: The marginal intervals of IMP convex variables.

	IMP convex variables			
Marginal intervals of μ_Δ	$\mu_{\Delta 1}$ $[0.0018^1, 0.0020^2]$	$\mu_{\Delta 2}$ $[0.0048^1, 0.0050^2]$	$\mu_{\Delta 3}$ $[0.0148^1, 0.0150^2]$	$\mu_{\Delta 4}$ $[0.0024^1, 0.0025^2]$
Marginal intervals of μ_Z	μ_{Z1} $[0.4^1, 0.5^2]$	μ_{Z2} $[0.6^1, 0.7^2]$	μ_{Z3} $[0.8^1, 1.1^2]$	μ_{Z4} $[1.2^1, 1.5^2]$

1: lower bound; 2: upper bound.
1 and 2 originated from FEMA 273 [54], FEMA 356 [55], and FEMA 445 [56].

Table 3: Results with N_2=1 by different methods.

Numerical methods	Failure probabilities in 50 years for different limit states				Function calls	Relative error*
	NO level	IO level	LS level	CP level		
MCS	10.260%	1.653%	0.170%	0.0739%	$2 \times 100 \times 10^5$	-
ALK-MGHAR	10.246%	1.647%	0.169%	0.0738%	63	0.135%
MPM	9.951%	1.599%	0.165%	0.0716%	283	3.11%
SLI	9.922%	1.598%	0.164%	0.0713%	147	3.52%

*: calculated relative error under CP level.

7.2. Reliability Analysis with Performance Function (15)

7.2.1. Case 1: $N_2 = 2$. If the parameter N_2 in (15) is greater than or equal to 2, the performance function will be nonlinear. In this section, (15) with N_2=2 is considered. Analogous to the performance function (16), 10^5 sampling points are generated and the minimal value of the Kriging model at each of the simulated samples is repeatedly explored to obtain the sign of the minimum function value. The sign of the extreme values predicted by ALK-MGHAR is shown in Figure 6. It can be observed that only 2 signs are wrongly predicted.

Based on different methods, the results are listed in Table 4. It is seen that both MPM and SLI obtain the precise results. Qin et al. (2007) revealed that the nonlinearity of the performance function could make FORM produce large errors in reliability analysis. In general, both MPM and SLI based on FORM may generate large errors for nonlinear problems. However, the performance function (15) with N_2=2 is not highly nonlinear and is monotonic with respect to the IMP convex variables defined in Section 3.2. Moreover, SLI is an effective method based on the assumption that the performance function is monotonic with respect to convex variables [35]. Therefore, the two methods and the proposed method behave very well in accuracy except in efficiency. ALK-MGHAR only requires 65 performance function computations that are less than 1/4 of MPM. This testifies the efficiency of the proposed method.

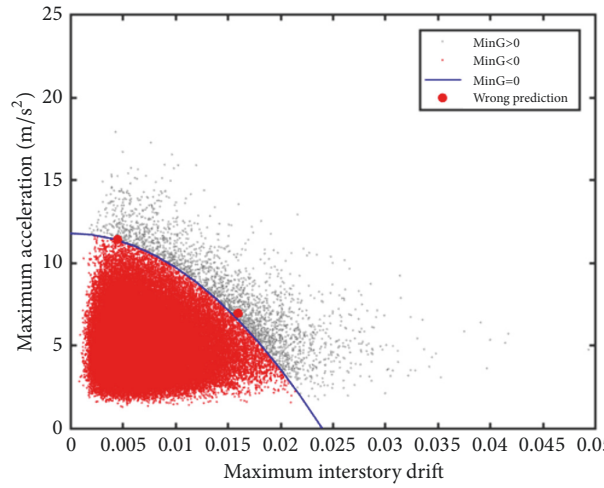

Figure 6: Sign of the minimum performance function with N_2=2 predicted by ALK-MGHAR.

7.2.2. Case 2: $N_2 \geq 2$. The parameter N_2 in (15) represents the nonlinearity of the performance function which reflects the limit state $G(\mathbf{X}, \boldsymbol{\mu}) = 0$. If N_2 is greater than or equal to 3, (15) will become a nonlinear function. Based on different methods, the results with different values of N_2 are listed in Table 5. It can be observed that both MPM and SLI provide results with a large error for this problem. The reason is that

Table 4: Results with N_2=2 by different methods.

Numerical methods	Failure probabilities in 50 years for different limit states				Function calls	Relative error*
	NO level	IO level	LS level	CP level		
MCS	6.339%	1.140%	0.120%	0.0596%	$2 \times 100 \times 10^5$	-
ALK-MGHAR	6.310%	1.136%	0.119%	0.0594%	65	0.34%
MPM	6.105%	1.099%	0.116%	0.0575%	301	3.55%
SLI	6.097%	1.097%	0.115%	0.0573%	159	3.83%

*: calculated relative error under CP level.

Table 5: Results with different values of N_2 by different methods.

N_2	Numerical method	Failure probabilities in 50 years under four levels				Function calls	Relative error*
		NO level	IO level	LS level	CP level		
N_2=3	MCS	5.67%	1.03%	0.098%	0.0424%	$2 \times 100 \times 10^5$	-
	ALK-MGHAR	5.652%	1.026%	0.0976%	0.0423%	68	0.338%
	MPM	4.145%	0.763%	0.0749%	0.0329%	327	22.34%
	SLI	4.347%	0.806%	0.0758%	0.0331%	161	22.03%
N_2=6	MCS	3.27%	0.71%	0.080%	0.0290%	$2 \times 100 \times 10^5$	-
	ALK-MGHAR	3.259%	0.708%	0.0797%	0.0288%	73	0.359%
	MPM	2.613%	0.559%	0.0623%	0.0226%	328	22.17%
	SLI	2.577%	0.546%	0.0624%	0.0223%	165	22.99%

*: calculated relative error under CP level.

the nonlinearity of (15) makes MPM generate a large error as stated in Section 7.2.1. Because the performance function (15) for different limit states defined by Section 6.3 is monotonic within a specified interval, the performance of SLI is similar to that of MPM. From Table 5, it is also observed that ALK-MGHAR only needs 68 calls to the performance function (15) related to N_2=3 and requires 73 function calls related to N_2=6. However, both MPM and SLI still need many calls to the performance function. This demonstrates that no matter in accuracy or efficiency, ALK-MGHAR exhibits much better than other different methods.

7.3. Reliability Analysis with Performance Function (14). When N_1 is equal to 3 and N_2 is equal to 4, (14) becomes a more highly nonlinear function. After the Kriging model is constructed, the optimization problem for the true function (14) is replaced by the optimization for the Kriging model. Then MCS can be performed based on the Kriging model. Likewise, 10^5 samples are generated and the optimization is implemented for each of the simulated samples. The sign of the minimum function value at each sample predicted by ALK-MGHAR is shown in Figure 7. It is observed that only 2 signs are wrongly predicted. That illustrates the accuracy of the Kriging model and verifies the applicability of the property provided in Section 5.1 to MGHAR.

Based on different methods, the results for this problem are listed in Table 6. It can be seen that both MPM and SLI obtain results with a large error. This is because the high nonlinearity of the performance function (14) with N_1=3 and N_2=4 makes FORM produce large errors. Both MPM and SLI proposed by Luo et al. [35] are based on FORM. The performance of SLI is still similar to that of MPM. From Table 6, it is also observed that ALK-MGHAR offers

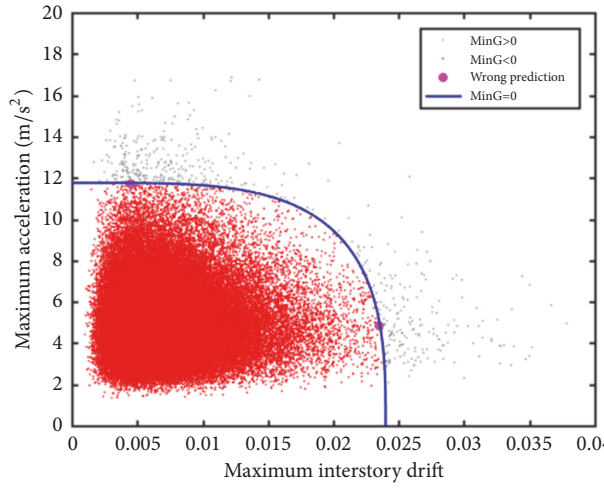

Figure 7: Sign of the minimum performance function with N_1=3 and N_2=4 predicted by ALK-MGHAR.

very precise results. This testifies that the nonlinearity of the performance function cannot affect the accuracy of the proposed method. Moreover, the computational cost of the proposed method is much less than that of both MPM and SLI. These findings demonstrate that ALK-MGHAR is suitable to deal with such complicated seismic engineering problems with strongly nonlinear performance functions.

8. Conclusions

This paper provides an ALK-MGHAR method. MGHAR investigated here represents the reliability problem of a given

Table 6: Results with N_1=3 and N_2=4 by different methods.

Numerical methods	Failure probabilities in 50 years for different limit states				Function calls	Relative error*
	NO level	IO level	LS level	CP level		
MCS	4.39%	0.95%	0.0892%	0.0355%	$2 \times 100 \times 10^5$	-
ALK-MGHAR	4.376%	0.946%	0.0880%	0.0354%	65	0.342%
MPM	2.858%	0.618%	0.0633%	0.0230%	321	34.89%
SLI	2.898%	0.627%	0.0636%	0.0234%	163	33.97%

*: calculated relative error under CP level.

RC structure with both random and IMP variables. Limit thresholds of different types of components are treated as random variables. The median of random variables is represented by an improved MP convex model, in which the uncertain domain of correlated bounded (interval) variables can be explicitly expressed by the matrix inequality. The corresponding EDPs are considered as dependent random variables and follow a multidimensional lognormal distribution. Through matrix transformation, the limit state function is mapped into the corresponding regularized one. The Kriging model is used to approximate the performance function in the region of interest rather than in the overall uncertain space. ALK-MGHAR starts its iterative process with constructing an initial Kriging model by defining an initial DoE with a handful of training points. The point at which the sign of the performance function has the maximum risk to be wrongly predicted should be added into DoE. Sequentially, the added point from candidate points is used to update the Kriging model. After the ALK model is constructed, a large amount of samples is generated and the optimization is implemented at each sample. Then, the maximum seismic failure probability for different limit states can be performed by using MCS. Further, the failure probabilities for different limit states in 50 years can be obtained through coupling the seismic failure probability and the ground motion hazard curve. To demonstrate the efficiency and accuracy of ALK-MGHAR, a six-story RC building is used as a case study. The interstory drift and the acceleration can be, respectively, obtained through IDA and NHA.

From this numerical example, it is demonstrated that the proposed method exhibits much better than other different methods such as MPM and SLI no matter in accuracy or in efficiency. Meanwhile, ALK-MGHAR is found capable of providing very accurate results for MGHAR and requires only a few of calls to the performance function. The phenomenon testifies that ALK-MGHAR only rightly predicting the sign of the performance function can meet the accurate requirement of MGHAR. It is also illustrated that ALK-MGHAR is able to deal with complex seismic engineering problems with strongly nonlinear performance functions.

Data Availability

No data were used to support this study.

Conflicts of Interest

The authors declare that they have no conflicts of interest.

Acknowledgments

Our authors acknowledge the support of National Natural Science Foundation of China (grant number 11802224), China Postdoctoral Science Foundation (grant number 2018M633495), Fundamental Research Funds for the Central Universities (3102016ZY2016), and Aerospace Science and Technology Innovation Fund (2016kc060013).

References

[1] V. Piluso, G. Rizzano, and I. Tolone, "Seismic reliability assessment of a two-story steel-concrete composite frame designed according to Eurocode 8," *Structural Safety*, vol. 31, no. 5, pp. 383–395, 2009.

[2] Z. H. Zeng, J. Fan, and Q. Q. Yu, "Performance-Based probabilistic seismic demand analysis of bridge structures," *Engineering Mechanics*, vol. 29, no. 3, pp. 156–162, 2012 (Chinese).

[3] K. A. Porter, "An overview of PEER's performance-based earthquake engineering methodology," in *Proceedings of 9th International Conference on Applications of Statistics and Probability in Civil Engineering*, San Francisco, California, USA, 2003.

[4] J. Moehle and G. G. Deierlein, "A framework methodology for performance-based earthquake engineering," in *Proceedings of 13th Word Conference on Earthquake Engineering*, Canadian Association for Earthquake Engineering, Vancouver, Canada, 2004.

[5] T. Y. Yang, J. Moehle, B. Stojadinovic, and A. Der Kiureghian, "Seismic performance evaluation of facilities: Methodology and implementation," *Journal of Structural Engineering*, vol. 135, no. 10, pp. 1146–1154, 2009.

[6] M. Khatibinia, M. J. Fadaee, J. Salajegheh, and E. Salajegheh, "Seismic reliability assessment of RC structures including soil-structure interaction using wavelet weighted least squares support vector machine," *Reliability Engineering & System Safety*, vol. 110, pp. 22–33, 2013.

[7] X. X. Liu, Z.-Y. Wu, and F. Liang, "Multidimensional performance limit state for probabilistic seismic demand analysis," *Bulletin of Earthquake Engineering*, vol. 14, no. 12, pp. 3389–3408, 2016.

[8] S. K. Ramamoorthy, P. Gardoni, and J. M. Bracci, "Probabilistic demand models and fragility curves for reinforced concrete frames," *Journal of Structural Engineering*, vol. 132, no. 10, pp. 1563–1572, 2006.

[9] B. R. Ellingwood, O. C. Celik, and K. Kinali, "Fragility assessment of building structural systems in Mid-America," *Earthquake Engineering & Structural Dynamics*, vol. 36, no. 13, pp. 1935–1952, 2007.

[10] O. C. Celik and B. R. Ellingwood, "Seismic risk assessment of gravity load designed reinforced concrete frames subjected to

mid-America ground motions," *Journal of Structural Engineering*, vol. 135, no. 4, pp. 414–424, 2009.

[11] N. Buratti, B. Ferracuti, and M. Savoia, "Response Surface with random factors for seismic fragility of reinforced concrete frames," *Structural Safety*, vol. 32, no. 1, pp. 42–51, 2010.

[12] J. Wieser, *Assessment of floor accelerations in yielding buildings. M.Sc.Thesis*, University of Nevada, Reno, USA, 2011.

[13] S. Soroushian, A. E. Zaghi, M. Maragakis, A. Echevarria, Y. Tian, and A. Filiatrault, "Seismic fragility study of fire sprinkler piping systems," in *Proceedings of the Structures Congress 2013: Bridging Your Passion with Your Profession*, pp. 1533–1544, USA, May 2013.

[14] Y. Tian, A. Filiatrault, and G. Mosqueda, "Experimental seismic study of pressurized fire sprinkler piping subsystems," Report MCEER-13-000, University at Buffalo, the State University of New York, Buffalo, NY, USA, 2013.

[15] C. A. Cornell, F. Jalayer, R. O. Hamburger, and D. A. Foutch, "Probabilistic basis for 2000 SAC federal emergency management agency steel moment frame guidelines," *Journal of Structural Engineering*, vol. 128, no. 4, pp. 526–533, 2002.

[16] F. Jalayer and A. Cornell, *A technical framework for probability-based demand and capacity factor (DCFD) seismic formats*, PEER Report: 2003/08. Pacific Earthquake Engineering Research Center, Berkeley: College of Engineering, University of California, 2003.

[17] L. Eads, E. Miranda, H. Krawinkler, and D. G. Lignos, "An efficient method for estimating the collapse risk of structures in seismic regions," *Earthquake Engineering & Structural Dynamics*, vol. 42, no. 1, pp. 25–41, 2013.

[18] D. G. Lü, X. H. Yu, F. Pan, and G. Y. Wang, "Probabilistic seismic demand analysis considering random system properties by an improved cloud method," in *Proceedings of the 14th World Conference on Earthquake Engineering*, Beijing, China, 2008.

[19] D. G. Lü, X. H. Yu, F. Pan, and G. Y. Wang, "Global probabilistic seisimic capacity analysis of structures based on MVFOSM finite element reliability method," *Word Earthquake Engineering*, vol. 24, no. 2, pp. 1–8, 2008.

[20] D. Lü, X. Yu, M. Jia, and G. Wang, "Seismic risk assessment for a reinforced concrete frame designed according to Chinese codes," *Structure and Infrastructure Engineering*, vol. 10, no. 10, pp. 1295–1310, 2014.

[21] Q. Y. Wu, H. P. Zhu, J. Fan, and Z. H. Zeng, "Seismic performance assessment on some frame structure," *Journal of Vibration and Shock*, vol. 31, no. 15, pp. 158–164, 2012.

[22] D. G. Lü, X. P. Li, F. Pan, and G. Y. Wang, "Global seismic reliability analysis of structures based on finite element reliability method and performance," *Journal of Natural Disasters*, vol. 15, no. 2, pp. 107–114, 2006.

[23] D. G. Lü, X. H. Yu, F. Pan, and G. Y. Wang, "Global probabilistic seisimic capacity analysis of structures based on FORM finite element reliability method," *Engineering Mechanics*, vol. 29, no. 2, pp. 1–7, 2012 (Chinese).

[24] P. Song, D. Lü, and S. Cui, "Reliability analysis of progressive collapse limit state of reinforced concrete frame structure under earthquakes," *Jianzhu Jiegou Xuebao/Journal of Building Structures*, vol. 34, no. 4, pp. 15–22, 2013.

[25] D. G. Lü, P. Y. Song, X. H. Yu, and G. Y. Wang, "Nonlinear global seismic reliability analysis of structures based on moment methods," *Journal of Building Structures*, vol. S2, pp. 119–124, 2010.

[26] P. Y. Song, *Structural global reliability methods and nonlinear global seismic reliability analysis of RC frames*, PHD thesis, Harbin Institute of Technology, Harbin, China, 2012.

[27] D. G. Lü, P. Y. Song, X. H. Yu, and G. Y. Wang, "Three mathematical models and solution methods for global seismic reliability analysis of structures," *Journal of Civil, Architectural and Environmental Engineering*, vol. 32, pp. 676–680, 2010.

[28] I. Elishakoff, "Essay on uncertainties in elastic and viscoelastic structures: from A. M. Freudenthal's criticisms to modern convex modeling," *Computers & Structures*, vol. 56, no. 6, pp. 871–895, 1995.

[29] I. Elishakoff, *Are probabilistic and anti-optimization approaches compatible? Whys and hows in uncertainty modelling*, Springer Vienna, New York, 1999.

[30] X. Wang, Z. Qiu, and I. Elishakoff, "Non-probabilistic set-theoretic model for structural safety measure," *Acta Mechanica*, vol. 198, no. 1-2, pp. 51–64, 2008.

[31] B. Möller and M. Beer, "Engineering computation under uncertainty - Capabilities of non-traditional models," *Computers & Structures*, vol. 86, no. 10, pp. 1024–1041, 2008.

[32] C. Jiang, X. Han, G. Y. Lu, J. Liu, Z. Zhang, and Y. C. Bai, "Correlation analysis of non-probabilistic convex model and corresponding structural reliability technique," *Computer Methods Applied Mechanics and Engineering*, vol. 200, no. 33–36, pp. 2528–2546, 2011.

[33] C. Jiang, R. G. Bi, G. Y. Lu, and X. Han, "Structural reliability analysis using non-probabilistic convex model," *Computer Methods Applied Mechanics and Engineering*, vol. 254, pp. 83–98, 2013.

[34] J. Guo and X. Du, "Sensitivity analysis with mixture of epistemic and aleatory uncertainties," *AIAA Journal*, vol. 45, no. 9, pp. 2337–2349, 2007.

[35] Y. J. Luo, Z. Kang, and A. Li, "Structural reliability assessment based on probability and convex set mixed model," *Computers & Structures*, vol. 87, no. 21-22, pp. 1408–1415, 2009.

[36] Z. P. Qiu and J. Wang, "The interval estimation of reliability for probabilistic and non-probabilistic hybrid structural system," *Engineering Failure Analysis*, vol. 17, no. 5, pp. 1142–1154, 2010.

[37] J. Guo and X. Du, "Reliability analysis for multidisciplinary systems with random and interval variables," *AIAA Journal*, vol. 48, no. 1, pp. 82–91, 2010.

[38] C. Jiang, G. Y. Lu, X. Han, and L. X. Liu, "A new reliability analysis method for uncertain structures with random and interval variables," *International Journal of Mechanics and Materials in Design*, vol. 8, no. 2, pp. 169–182, 2012.

[39] W. Yao, X. Chen, Y. Huang, and M. Van Tooren, "An enhanced unified uncertainty analysis approach based on first order reliability method with single-level optimization," *Reliability Engineering & System Safety*, vol. 116, pp. 28–37, 2013.

[40] J. Guo and X. Du, "Reliability sensitivity analysis with random and interval variables," *International Journal for Numerical Methods in Engineering*, vol. 78, no. 13, pp. 1585–1617, 2009.

[41] P. Wang, Z. Lu, and Z. Tang, "An application of the Kriging method in global sensitivity analysis with parameter uncertainty," *Applied Mathematical Modelling: Simulation and Computation for Engineering and Environmental Systems*, vol. 37, no. 9, pp. 6543–6555, 2013.

[42] Y. Zhang, Y. Liu, X. Yang, and Z. Yue, "A global nonprobabilistic reliability sensitivity analysis in the mixed aleatory-epistemic uncertain structures," *Proceedings of the Institution of Mechanical Engineers, Part G: Journal of Aerospace Engineering*, vol. 228, no. 10, pp. 1802–1814, 2014.

[43] Y. Zhang, Y. Liu, X. Yang, and B. Zhao, "An efficient Kriging method for global sensitivity of structural reliability analysis with non-probabilistic convex model," *Proceedings of the Institution of Mechanical Engineers, Part O: Journal of Risk and Reliability*, vol. 229, no. 5, pp. 442–455, 2015.

[44] X. Yang, Y. Liu, Y. Zhang, and Z. Yue, "Hybrid reliability analysis with both random and probability-box variables," *Acta Mechanica*, vol. 226, no. 5, pp. 1341–1357, 2015.

[45] X. F. Yang, Y. S. Liu, Y. Gao, Y. S. Zhang, and Z. Z. Gao, "An active learning kriging model for hybrid reliability analysis with both random and interval variables," *Structural and Multidisciplinary Optimization*, vol. 51, no. 5, pp. 1003–1016, 2015.

[46] Q. Qin, D. Lin, G. Mei, and H. Chen, "Effects of variable transformations on errors in FORM results," *Reliability Engineering & System Safety*, vol. 91, no. 1, pp. 112–118, 2006.

[47] B. Echard, N. Gayton, and M. Lemaire, "AK-MCS: an active learning reliability method combining Kriging and Monte Carlo simulation," *Structural Safety*, vol. 33, no. 2, pp. 145–154, 2011.

[48] A. Dumas, B. Echard, N. Gayton, O. Rochat, J.-Y. Dantan, and S. Van Der Veen, "AK-ILS: An active learning method based on Kriging for the inspection of large surfaces," *Precision Engineering*, vol. 37, no. 1, pp. 1–9, 2013.

[49] C. Jiang, Q. F. Zhang, X. Han, and Y. H. Qian, "A non-probabilistic structural reliability analysis method based on a multidimensional parallelepiped convex model," *Acta Mechanica*, vol. 225, no. 2, pp. 383–395, 2014.

[50] C. Jiang, Q. F. Zhang, X. Han, J. Liu, and D. A. Hu, "Multidimensional parallelepiped model—a new type of non-probabilistic convex model for structural uncertainty analysis," *International Journal for Numerical Methods in Engineering*, vol. 103, no. 1, pp. 31–59, 2015.

[51] C. Jiang, C.-M. Fu, B.-Y. Ni, and X. Han, "Interval arithmetic operations for uncertainty analysis with correlated interval variables," *Acta Mechanica Sinica*, pp. 1–10, 2015.

[52] B. Y. Ni, C. Jiang, and X. Han, "An improved multidimensional parallelepiped non-probabilistic model for structural uncertainty analysis," *Applied Mathematical Modelling*, vol. 40, no. 7-8, pp. 4727–4745, 2016.

[53] H. B. Sun, Z. Y. Wu, and X. X. Liu, "Multidimensional performance limit state for structural fragility estimation," *Engineering mechanics*, vol. 30, no. 5, pp. 147–152, 2013.

[54] FEMA 273, *NEHRP Guidelines for the seismic rehabilitation of buildings*, Federal Emergency Management Agency, Washington, DC, USA, 1997.

[55] FEMA 356, *Prestandard and commentary for the seismic rehabilitation of buildings*, Federal Emergency Management Agency, Washington, DC, USA, 2000.

[56] FEMA 445, *Next-generation performance-based seismic design guidelines: program plan for new and existing buildings*, ATC for the Federal Emergency, Washington, DC, USA, 2006.

[57] P.-L. Liu and A. der Kiureghian, "Multivariate distribution models with prescribed marginals and covariances," *Probabilistic Engineering Mechanics*, vol. 1, no. 2, pp. 105–112, 1986.

[58] M. Rosenblatt, "Remarks on a multivariate transformation," *Annals of Mathematical Statistics*, vol. 23, pp. 470–472, 1952.

[59] A. D. Kiureghian, "Non-ergodicity and PEER's framework formula," *Earthquake Engineering & Structural Dynamics*, vol. 34, no. 13, pp. 1643–1652, 2005.

[60] G. P. Cimellaro and A. M. Reinhorn, "Multidimensional performance limit state for hazard fragility functions," *Journal of Engineering Mechanics*, vol. 137, no. 1, 2010.

[61] J. M. Gablonsky, "Implementation of the DIRECT Algorithm, Center for Research in Scientic Computation," Tech. Rep., Technical Report CRSC-TR98-29, North Carolina State University, Raleigh, NC, USA, 1998.

[62] Z. Kang and Y. Luo, "Reliability-based structural optimization with probability and convex set hybrid models," *Structural and Multidisciplinary Optimization*, vol. 42, no. 1, pp. 89–102, 2010.

[63] Y. Luo, A. Li, and Z. Kang, "Reliability-based design optimization of adhesive bonded steel-concrete composite beams with probabilistic and non-probabilistic uncertainties," *Engineering Structures*, vol. 33, no. 7, pp. 2110–2119, 2011.

[64] X. Yang, Y. Liu, Y. Zhang, and Z. Yue, "Probability and convex set hybrid reliability analysis based on active learning Kriging model," *Applied Mathematical Modelling*, vol. 39, no. 14, pp. 3954–3971, 2015.

[65] Z. Sun, J. Wang, R. Li, and C. Tong, "LIF: A new Kriging based learning function and its application to structural reliability analysis," *Reliability Engineering & System Safety*, vol. 157, pp. 152–165, 2017.

[66] H. Zhao, Z. Yue, Y. Liu, Z. Gao, and Y. Zhang, "An efficient reliability method combining adaptive importance sampling and Kriging metamodel," *Applied Mathematical Modelling: Simulation and Computation for Engineering and Environmental Systems*, vol. 39, no. 7, pp. 1853–1866, 2015.

[67] Z. Lv, Z. Lu, and P. Wang, "A new learning function for Kriging and its applications to solve reliability problems in engineering," *Computers & Mathematics with Applications. An International Journal*, vol. 70, no. 5, pp. 1182–1197, 2015.

[68] X. Yang, Y. Liu, and Y. Gao, "Unified reliability analysis by active learning Kriging model combining with random-set based Monte Carlo simulation method," *International Journal for Numerical Methods in Engineering*, vol. 108, no. 11, pp. 1343–1361, 2016.

[69] D. R. Jones, M. Schonlau, and W. J. Welch, "Efficient global optimization of expensive black-box functions," *Journal of Global Optimization*, vol. 13, no. 4, pp. 455–492, 1998.

[70] G. Matheron, "The intrinsic random functions and their applications," *Advances in Applied Probability*, vol. 5, pp. 439–468, 1973.

[71] A. Tavassoli, K. Haji Hajikolaei, S. Sadeqi, G. G. Wang, and E. Kjeang, "Modification of DIRECT for high-dimensional design problems," *Engineering Optimization*, vol. 46, no. 6, pp. 810–823, 2014.

[72] GB50011, *GB50011-2010. Code for seismic design of buildings*, China Architecture Industry Press, Beijing of China, 2010.

[73] JGJ3, "Technical specification for concrete structures of tall building," Tech. Rep., China Architecture Industry Press, Beijing of China, 2010.

[74] S. Mazzoni, F. McKenna, M. H. Scott, and G. L. Fenves, *OpenSees command language manual*, C. A. Berkeley, Ed., vol. 10, Pacific Earthquake Engineering Research Center, University of California at Berkeley, Berkeley, CA, USA, 2006, http://opensees.berkeley.edu/.